Received: 30 January 2023 | Revised: 22 December 2023 | Accepted: 29 December 2023

DOI: 10.1002/ijc.34859

IJC INTERNATIONAL JOURNAL of CANCER

RESEARCH ARTICLE

Tumor Immunology and Microenvironment

SAA1-dependent reprogramming of adipocytes by tumor cells is associated with triple negative breast cancer aggressiveness

Ilona Rybinska[1] | Nunzia Mangano[1] | Sandra L. Romero-Cordoba[2,3] | Viola Regondi[1] | Valentina Ciravolo[1] | Loris De Cecco[4] | Elisa Maffioli[5,6] | Biagio Paolini[7] | Francesca Bianchi[8] | Lucia Sfondrini[1,8] | Gabriella Tedeschi[5,6] | Roberto Agresti[9] | Elda Tagliabue[1] | Tiziana Triulzi[1]

[1]Microenvironment and Biomarkers of Solid Tumors Unit, Department of Experimental Oncology, Fondazione IRCCS Istituto Nazionale dei Tumori di Milano, Milan, Italy

[2]Departamento de Medicina Genómica y Toxicología Ambiental, Instituto de Investigaciones Biomédicas, Universidad Nacional Autónoma de México, Mexico City, Mexico

[3]Departamento de Bioquímica, Instituto Nacional de Ciencias Médicas y Nutrición "Salvador Zubirán", Mexico City, Mexico

[4]Molecular Mechanisms Unit, Department of Experimental Oncology, Fondazione IRCCS Istituto Nazionale dei Tumori di Milano, Milan, Italy

[5]Dipartimento di Medicina Veterinaria e Scienze Animali, Università degli Studi di Milano, Milano, Italy

[6]CIMAINA, Università degli Studi di Milano, Milano, Italy

[7]Anatomic Pathology A Unit, Department of Pathology, Fondazione IRCCS Istituto Nazionale dei Tumori di Milano, Milan, Italy

[8]Department of Biomedical Science for Health, Università degli Studi di Milano, Milan, Italy

[9]Division of Surgical Oncology, Breast Unit, Fondazione IRCCS Istituto Nazionale dei Tumori di Milano, Milan, Italy

Correspondence
Tiziana Triulzi, Microenvironment and Biomarkers of Solid Tumors Unit, Department of Experimental Oncology, Fondazione IRCCS Istituto Nazionale dei Tumori di Milano, Via G. Amadeo, 20133 Milan, Italy.
Email: tiziana.triulzi@istitutotumori.mi.it

Funding information
Fondazione AIRC, Grant/Award Numbers: IG 2016—ID 18712, IG 2020—ID 24984, TRIDEO 2014—ID 16117

Abstract

Triple negative breast cancers (TNBC) are characterized by a poor prognosis and a lack of targeted treatments. Their progression depends on tumor cell intrinsic factors, the tumor microenvironment and host characteristics. Although adipocytes, the primary stromal cells of the breast, have been determined to be plastic in physiology and cancer, the tumor-derived molecular mediators of tumor-adipocyte crosstalk have not been identified yet. In this study, we report that the crosstalk between TNBC cells and adipocytes in vitro beyond adipocyte dedifferentiation, induces a unique transcriptional profile that is characterized by inflammation and pathways that are related to interaction with the tumor microenvironment. Accordingly, increased cancer stem-like features and recruitment of pro-tumorigenic immune cells are induced by this crosstalk through CXCL5 and IL-8 production. We identified serum amyloid A1 (SAA1) as a regulator of the adipocyte reprogramming through CD36 and P2XR7 signaling. In human TNBC, SAA1 expression was associated with cancer-associated adipocyte infiltration, inflammation, stimulated lipolysis, stem-like properties, and a distinct tumor immune microenvironment. Our findings constitute

Ilona Rybinska and Nunzia Mangano contributed equally to this study.

evidence that the interaction between tumor cells and adipocytes through the release of SAA1 is relevant to the aggressiveness of TNBC.

KEYWORDS
cancer-associated adipocytes, gene expression profile, inflammation, SAA1, triple negative breast cancer

What's new?

Adipocytes are suspected of playing a role in breast cancer progression, with increasing evidence that adipocytes interact with tumor cells. Potential mechanisms underlying such interactions, however, remain unknown. Here, mechanisms of crosstalk involving adipocytes and triple negative breast cancer (TNBC) cells were investigated in vitro. Experiments identified serum amyloid A1 (SAA1) as a regulator of TNBC cell-induced adipocyte modification. SAA1 expression in human TNBCs was associated with the expression of a cancer-associated adipocyte signature and with aggressive tumor features found to be regulated by adipocytes in cellular models. The findings cast new light on relationships between adipocytes and TNBC progression.

1 | INTRODUCTION

Breast cancer (BC) is the most frequent cancer among women and a leading cause of cancer-related mortality worldwide.[1] Triple-negative breast cancer (TNBC) is a particularly aggressive molecular BC subtype that is characterized by absence of estrogen and progesterone receptors and the HER2 oncoprotein, lacking targeted therapies. Moreover, like BC in general, considerable biological heterogeneity within TNBC exists[2,3] translating into differences in patient outcomes and potential responses to therapies.[3,4]

Cancer development and progression depend on tumor cell-intrinsic factors, the tumor microenvironment, and host characteristics. Adipocytes, the primary stromal cells in the breast, have been implicated in the progression of BC by epidemiological studies that have reported associations between obesity, an increased risk of cancer, and a poor prognosis,[5] and breast tumors often metastasize to adipose-rich niches, such as the brain and bone marrow.[6] Additionally, during mammary gland development, breast adipocytes become susceptible to physiological signals, leading to their cyclical dedifferentiation into preadipocyte-like precursors and redifferentiation into adipocytes.[7]

Interactions between BC cells and adipocytes have been described in vitro, resulting in alteration to both cell types.[8,9] Adipocytes modify their phenotype by decreasing the expression of differentiation markers and lipid content, and like cancer-associated fibroblasts, they have been called cancer-associated adipocytes (CAAs).[10] CAAs, similarly to adipocytes in obesity, influence tumor cell metabolism and aggressiveness by increasing proinflammatory molecule secretion, inducing extracellular matrix (ECM) remodeling, and changing their metabolism.[5] Recently, the contribution of tumor-induced adipocyte reprogramming to cancer progression was also demonstrated in vivo.[11] However, the key drivers of this process have not been identified.[11,12]

Serum amyloid A1 (SAA1), a well-known acute phase protein that is produced in the liver, is expressed in the epithelial components and stromal cells of many normal extrahepatic tissues, including the breast,[13] and in several tumor cell types and components of the tumor microenvironment.[14] Its serum and tissue levels are significantly higher in several malignancies, including BC,[15] and correlate with a poor prognosis.[14] In addition, various studies have shown that SAA1 contributes to cancer progression by promoting proliferation, metastasis, inflammation, and angiogenesis.[16–21] In the current study, we examined the molecular mechanisms of the interaction between TNBC cells and adipocytes, identifying a new function of tumor-derived SAA1.

2 | METHODS

2.1 | Patients

Adipose tissues (ATs) were collected for gene expression profiling at Fondazione IRCCS Istituto Nazionale dei Tumori (INT) of Milan, from patients who were undergoing mastectomy. Tumor-adjacent AT was taken within 2 cm of the tumor and tumor-distant AT was sampled peripherally, at the opposite site, from more than 10 cm away from the tumor. Samples were collected during standard surgical and medical procedures at INT and donated by patients to the Institutional Bio-Bank, for research purposes.

2.2 | Cell culture

Human BC cell lines, ASC52telo human adipose-derived mesenchymal stem cells (MSCs, RRID:CVCL-U602), 3T3-L1 murine preadipocytes (RRID:CVCL-0123), and 4T1 murine mammary carcinoma cells (RRID:

CVCL-0125) were obtained from ATCC. All cell lines were grown in a humidified chamber (95% air, 5% CO_2) at 37°C. The human cell lines have been authenticated by STR profiling within the last 3 years. All experiments were performed with mycoplasma-free cells, as evaluated by the MycoAlert™ PLUS Mycoplasma detection kit (Lonza). MCF7 (RRID:CVCL-0031), T47-D (RRID:CVCL-0553), SK-BR-3 (RRID:CVCL-0033), HCC1954 (RRID:CVCL-1259), MDA-MB-231 (RRID:CVCL-0062), BT-549 (RRID:CVCL-1092), HCC1937 (RRID:CVCL-0290) and 4T1 cells were cultured in Roswell Park Memorial Institute (RPMI) 1640 Medium (Gibco, 16000-044); BT-474 (RRID:CVCL-0179), MDA-MB-361 (RRID:CVCL-0620) and MDA-MB-468 cells (RRID:CVCL-0419) were cultured in Dulbecco's Modified Eagle Medium (DMEM, Gibco, 41964–039); ZR-75-30 (RRID:CVCL-1661), SUM149PT (RRID:CVCL-3422) and SUM159PT cells (RRID:CVCL-5423) were cultured in DMEM-F12 (Gibco, 31331–028) that was supplemented with 5 µg/mL insulin (Sigma-Aldrich, I0516). Each media was supplemented with 10% fetal bovine serum (FBS, Gibco, 16000). ASC52 cells were cultured in MesenPRO RS™ (GIBCO, 12746012) supplemented with 2 mM glutamine (Lonza, BE17 605E), and 3T3-L1 cells were cultured in DMEM supplemented with sodium pyruvate to a final concentration of 1 mM (NaPyr, Lonza™ BioWhittaker™, BE13-115E).

The differentiation of mature adipocytes (MAs) was performed by seeding ASC52 cells in a 24-well plate (30,000 cells/well). After 72 h, the cells were treated with StemPRO® Adipogenesis Differentiation Medium (GIBCO, A1007001), which was changed twice per week until Day 14. Adipocyte modification was evaluated after culturing previously differentiated MAs in tumor cell-conditioned media (CM) or in co-culture with MDA-MB-231 cells in a Boyden chamber with a 0.4-µm filter (Corning, 3470) for 7 days by Oil Red O staining and qRT-PCR.

To produce BC cell CM, cells were seeded (2.6×10^6 cells per T25 flask) in their respective culture media. On the following day, the cells were rinsed and the medium was replaced with 10% FBS-containing RPMI and conditioned for 72 h. For the mass spectrometry analysis RPMI without FBS was used to obtained BC cell CM. The CM was centrifuged and frozen immediately at −80°C. To evaluate the effect of SAA1 on adipocytes, MAs were cultured in MDA-MB-231 CM or control media (RPMI with 10% FBS) in the presence of inhibitors (10 µM KN62 [Merck Life Science, I2142], 10 µM hexarelin [CliniSciences, OPPA01052], 50–200 µM Sulfosuccinimidyl Oleate [sodium salt] [SSO, Cayman chemical, 11211], 1 mg/mL anti-TLR2 [eBioscience, 16-9922-82], 1 mg/mL anti-TLR4 [eBioscience, 16-9917-82], 20 µM ST616792 [MedChemExpress, 56921], 100 µM PDTC [Merck Life Science, P8765], 1 µM BAY11-7082 [Santa Cruz Biotechnology, sc-202490]; 10 µM UO126 [Merck Life Science, 19147], 10 µM SP600125 [Merck Life Science, S5567]) or diluents for 48 h and then in RPMI with 10% FBS for an additional 5 days. The same treatments were applied to ASC52 MAs that were cultured in RPMI with or without 20 ng/mL hSAA1 (LSBio, LS-G318), as described.[22] RNA was obtained from cells at Day 7, whereas protein extraction for western blot was performed 48 h after treatment.

Detailed protocols for the Oil Red O staining, cell proliferation, CM characterization, and mass spectrometry analysis are provided in Supplementary Methods.

2.3 | SAA1 silencing

Gene-specific small interfering RNAs (siRNAs; SAA1-1: 5-AGGGTACACAATGGGTATCTA-3, SAA1-2: 5-TTACATCGGCTCAGACAAATA-3, Qiagen, SI04201526 and SI04151287, respectively) and negative control siRNA duplexes that targeted a non-coding sequence (scramble, siRNA) (5-AATTCTCCGAACGTGTCACGT-3, Qiagen, 1027310) were used. Transient transfection of siRNAs (50 nM) was performed using Lipofectamine RNAiMax (Invitrogen, 13778150), per the manufacturer's protocol, in Opti-MEM medium (Gibco, 11058021).

2.4 | RNA extraction and qRT-PCR

Total RNA was extracted from cell lines using Direct-zol™ RNA MicroPrep/MiniPrep isolation kits (Zymo Research, R2051/R2061). qRT-PCR was performed using Applied Biosystems™ Fast SYBR™ Green Master Mix 2X (Thermo Fisher Scientific, 4385612) or Applied Biosystems™ TaqMan Universal Master Mix 2X (Thermo Fisher Scientific, 4352042), on the StepOne Plus™ Real-time PCR instrument (Thermo Fisher Scientific), as described.[23] Beta-actin (*ACTB*) and beta-2 microglobulin (*B2M*) were used as endogenous controls for BCs and adipocytes, respectively. Relative mRNA concentrations were calculated by ddCt method. Details on the primers that were used are listed in Supplementary Table S1.

2.5 | Western blot analysis

Cell lysates were prepared in ice-cold TNTG buffer, as described.[24] Protein concentrations were measured with Coomassie Plus™ Protein Assay Reagent (Thermo Scientific, 1856210). A total of 25 µg and 20 µg protein from CM and cell lysates, respectively, were subjected to SDS-PAGE (NuPAGE 4–12% Bis-Tris gel, Invitrogen, NP0335BOX). Cell protein fractions were transferred to polyvinylidene difluoride (PVDF) membranes (Immobilon Membrane, IPVH00010), which were then blocked with 5% milk (GeneSpin, STS-M500) in Tri-buffered saline (TBS) that contained 0.1% Triton X-100 (TBST) (EMD Millipore Corporation, 9036-19-5), and incubated with primary antibodies diluted in 3% milk in TBST overnight at 4°C. See Supplementary Methods for the antibodies that were used. Proteins were detected by enhanced chemiluminescence (Pierce® ECL Western Blotting Substrate, Thermo Scientific, 32209). Vinculin was used as loading control. Band intensities were quantified in Quantity One® 1D (Bio-Rad).

2.6 | Migration assay and FACS

Human peripheral blood mononuclear cells, pooled with granulocytes from healthy donors, that were purified by density-gradient separation using Ficoll-Paque Premium (GE Healthcare, 17-5442-03), were subjected to 6 h migration assay using a Boyden chamber with a 3-µm filter (Corning, 3415). CM, derived from MAs or CAAs, was used

as the chemoattractant. Cells that migrated into the lower chamber were counted on a BD Accuri Flow Cytometer (BD Biosciences) and stained by direct immunofluorescence. Migration assay was also performed in the presence of a combination of neutralizing antibodies against IL-8 (0.08 µg/mL, R&D Systems, MAB208) and CXCL5 (0.3 µg/mL, R&D Systems, MAB254) or isotype control antibodies (0.4 µg/mL, R&D Systems, MAB002). The following antibodies were used to stain migrated human leukocytes: CD3VioGreen (Miltenyi Biotec, REA6/3), CD8VioBlue (Miltenyi Biotec, REA734), CD4FITC (Miltenyi Biotec, REA623), CD19FITC (BD Biosciences, HIB19), CD56APC (Miltenyi Biotec, REA196), CD14VioBlue (Miltenyi Biotec, REA599), CD15PE (Miltenyi Biotec, VIMC6), and CD16PerCP-Vio700 (Miltenyi Biotec, REA423). Samples were analyzed by gating live cells, labeled using the LIVE/DEAD fixable Near-IF stain kit (Invitrogen, L10119), after doublet exclusion (the gating strategy is shown in Supplementary Figure S3), on a FACSCelesta (BD Bioscience) and FlowJo (Tree Star Inc.).

2.7 | Gene expression profiling and analysis

Fifty-six AT samples (matched tumor-adjacent and tumor-distant samples from 28 normal-weight BC patients) and 15 ASC52 samples were analyzed. The data were deposited into the Gene Expression Omnibus repository (accession numbers GSE153316 and GSE153317, respectively).

RNA was obtained from ASC52 cells, using the miRNeasy Mini Kit (Qiagen, 217004) and from frozen adipose tissue (AT) using the RNeasy Lipid Tissue Mini Kit (Qiagen, 74804), according to the manufacturer's instructions. RNA concentrations were determined on a Qubit fluorometer (Thermo Fisher Scientific), and RNA quality was verified using TapeStation 4200 (Agilent). Gene expression profiles were generated by Affymetrix Clariom S Pico assay (Thermo Fisher Scientific), following the manufacturers protocol. Single-stranded cDNA samples for hybridization were generated from 100 ng of total RNA. The resulting cDNA was enzymatically fragmented and biotinylated, using the GeneChip™ WT Terminal Labeling kit (Thermo Fisher Scientific), mixed with hybridization buffer, and subjected to the Human Clariom S array, targeting >20,000 well-annotated genes. Arrays were stained on an Affymetrix GeneChip® Fluidics Station 450 and scanned on a 7G Affymetrix GeneChip® Scanner 3000. Raw data were processed using the Transcriptome Analysis Console (TAC; Thermo Fisher Scientific). CEL files, containing feature intensity values, were converted into summarized expression values, by Robust Multi-array Average (RMA)—which consists of background adjustment, quantile normalization, and summarization—across all chips. All samples passed quality control thresholds for hybridization, labeling, and the expression of housekeeping gene controls.

Bioinformatic data analyses were performed using TAC v4.2.0. Differentially expressed genes (DEGs) were identified using the limma package. Functional annotations of DEGs (false discovery rate [FDR] <0.1) was performed by enrichment analysis, based on a predefined biological process gene set from Gene Ontology (GO) annotation (http://bioinf.wehi.edu.au/software/MSigDB/index.html), using DAVID Bioinformatics Resources v6.8 and GSEA v4.0.3. CAA-specific genes were represented by the common DEGs between CAAs vs. MAs and CAAs vs. MSCs (FC >1.5, FDR <0.1, $n = 543$). CAAs features that were shared with MSCs were identified by analyzing the shared DEGs between MSCs vs. MAs and MAs vs. CAAs with opposite expression patterns (i.e., upregulated in the former and downregulated in the latter comparison) (FC >1.5, FDR <0.1, $n = 584$).

Enrichment maps of enriched gene sets (FDR <0.1) were obtained in Cytoscape v3.8.0 and cluster annotated with Auto Annotate app v1.3.2. We also assessed the association of ad hoc gene sets (i.e., the ASC52 CAA gene set, consisting of genes that were significantly upregulated in CAAs vs. MAs [FC >2, FDR < .1, Supplementary Table S2] by GSEA run in pre-rank mode, according to significance and fold-change by paired differential expression analysis of tumor-adjacent vs. tumor-distant AT samples). Enrichment was considered to be significant at $p < .05$.

2.8 | Mining TNBC gene expression profiles and data processing

We downloaded and evaluated publicly available data from 10 tumor data sets, profiled on Affymetrix platforms and deposited in the Gene Expression Omnibus database (GEO: GSE76250, GSE102484, GSE76275, GSE25066, GSE19615, GSE2603, GSE21653, GSE86945, GSE86946); RNA sequencing data available through The Cancer Genome Atlas (GDC TCGA Breast Cancer RNA counts) from the Xena browser; and normalized data from the METABRIC study,[25] recovered through cBioportal, for a total of 1311 TNBCs. Reported ER, PR, and HER2 immunohistochemical status was used to define the triple negative phenotype. Tumor purity was inferred according to the ESTIMATE algorithm.[26] Lehmann TNBC subtypes[2] were inferred via the web-based tool "TNBC type." A differentiation predictor[27] was applied based on available R commands. The CEMiTool[28] package was used. Immune infiltration landscape was defined using the CIBERSORTx web tool (https://cibersortx.stanford.edu/), the xCell tool (http://xcell.ucsf.edu/), and single-sample GSEA (ssGSEA) with published immune signatures.[29]

SAA1 classes, based on SAA1 mRNA expression, were defined as follows: SAA1-low, *SAA1* <1st quantile; SAA1-medium, >1st quantile and <3rd quantile; and SAA1-high, >3rd quantile. Details are provided in Supplementary Methods.

2.9 | Generation and application of a CAA signature

To robustly identified genes that subtype CAA content, we first determined useful genes using two approaches. First, we excluded genes that were significantly enriched in tumor samples by downloading data from the TCGA BC cohort and computing the relative expression of each gene in tumor samples by *z*-score. Higher positive *z*-scores were discarded. Second, we filtered genes that were differentially

expressed (lgFC >0.3, p <.05) between tumor-adjacent AT and tumor-distant AT. Feature selection was performed using the following computational platforms: Boruta (random forest with conditional inference trees), dtangle, Elastic net, sigFeature, and SVM-RFE, based on the most variable genes among the evaluated samples, as computed by MAD ($n = 2500$). The core of the classification module was implemented in the R environment.

To ensure the robustness of our results, the optimal number of features was determined by cross-algorithm calling; thus, only genes that were identified by at least 4 of the implemented tools were selected for incorporation into our classification model, defined as the minimum number of transcripts that classified samples as being enriched in tumor-adjacent AT tissue with the smallest error (CAA signature: *PROX1*, *MMRN1*, *FHL2*, *RGS16*, *THBS3*, *WEE1*, *PKHD1L1*, *NT5E*, *ASPN*, *C4A*, *C4B*, *CTGF*, *RUNX1*, *CCL21*, *SLC43A3*, *SERPINE1*, *KLF6*, *CRIP1*, *ITGB8*, *PIK3C2G*, *TPBG*, *OR52I2*). Next, TNBC expression profiles from the mining cohorts were adjusted by tumor purity using a linear regression model in the limma package. Adjusted gene expression was computed by ssGSEA method by GSVA in the R environment to score feature-selected genes that had been identified for CAA. CAA classes were defined as follows: CAA-low, CAA <1st quantile; CAA-medium, >1st quantile and <3rd quantile; and CAA-high, >3rd quantile.

2.10 | Statistics

Differences between groups were analyzed by two-tailed Student's *t*-test. Associations between categorical variables were analyzed by Fisher's exact test, and correlations between continuous variables were examined by Pearson correlation. Two-sided $p < .05$ was considered significant. Statistical analyses were performed using the GraphPad Prism 5.01 package (GraphPad).

3 | RESULTS

3.1 | Tumor-modified adipocytes are characterized by pro-tumoral features

To determine the molecular mechanisms of the interaction between tumor cells and adipocytes, we induced human ASC52 cells adipose-derived mesenchymal stem cells (MSCs) to become mature adipocytes (MAs) and treated them with or without conditioned media (CM) from human TNBC MDA-MB-231 cells. On incubation with tumor CM, ASC52 adipocytes decreased their lipid content and acquired and elongated fibroblast-like morphology (Figure 1A,B). Similar reduction in adipocyte lipid content was observed treating adipocytes with tumor 72 h CM, following the resuspension of the retained fraction from a 3 kDa centrifugal filter in fresh medium, tumor 24 h CM and 72 h CM diluted 1:2 with fresh medium (Supplementary Figure S1A). CAAs were characterized by the significant downregulation of adipocyte markers, including the peroxisome proliferator-activated receptor gamma (PPARG), adiponectin (ADIPOQ), and fatty acid-binding protein 4 (FABP4) at the mRNA (Figure 1C and Supplementary Figure S1B) and protein levels (Figure 1D) and by increased expression of the fibroblast markers alpha smooth muscle actin A (α-SMA) and platelet growth factor receptor beta (PDGFRβ, Figure 1D). The upregulation of α-SMA and PDGFRβ in CAAs compared to MAs and MSCs was confirmed by flow cytometry, as for PDGFRα (Figure 1E and Supplementary Figure S1C). Fibroblast Activation Protein (FAP) expression was high in ASC52 cells regardless of their differentiation stage (Supplementary Figure S1C). Similar changes were inducible in adipocytes by direct co-culture with MDA-MB-231 cells (Figure 1F) and by treatment with the CM of other TNBC cells (SUM149PT, MBA-MB-468, BT-549, HCC1937, Figure 1G), indicating that TNBC cells communicate with adipocytes in vitro.

To identify unique potential protumoral features of tumor-modified adipocytes, the transcriptomic profiles of ASC52 cells, which engender adipocytes, MAs and adipocytes that were modified by MDA-MB-231 CM (CAAs) were compared. By principal component analysis we noted a clear distinction in transcriptional profiles between MSCs, MAs, and CAAs (Figure 2A). Comparison of CAAs and MAs profiles yielded 1480 significant differentially expressed genes (DEGs) (Figure 2B) that were enriched in several biological processes, including cell cycle, metabolic process, ion transport, cytokine pathway, leukocyte migration, and cell adhesion (Figure 2C).

Specifically, ion transport, inflammation, and leukocyte migration were significantly enriched in CAA-specific genes (see Section 2.7, $n = 543$, Figure 2D). As expected, metabolic pathways that were related primarily to lipid metabolism, low response to insulin, high glutamine release, and amino acid metabolism, and pathways related to enhanced cell growth and ECM organization characterized CAA genes that were shared with MSCs (Figure 2E). Notably, by GSEA, CAA-specific genes (the ASC52 CAA gene set, Supplementary Table S2) were significantly positively enriched in tumor-adjacent adipose tissue (AT) compared with BC-distant AT from 28 patients (Figure 2F and Supplementary Table S2). These data indicate that tumor crosstalk with adipocytes did not only merely induce a return in the adipocyte differentiation process but also imparts distinct and novel characteristics onto adipocytes, making CAAs unique. Notably, these unique features of CAAs were validated in tumor-adjacent AT in patients.

3.2 | Cancer-associated adipocytes increase tumor cell stemness

To determine whether the unique properties of CAAs impact tumor aggressiveness, we treated MDA-MB-231 cells with CM that was derived from ASC52 MSCs, MAs, and CAAs. The CM from all ASC52 cells significantly favored BC cell proliferation, compared with cells that were maintained in control medium (Supplementary Figure S2A). However, cell proliferation was similar between CM, indicating that CAAs do not have specific effects on cancer cell proliferation.

Because inflammation and dysregulated lipid metabolism can induce epithelial-to-mesenchymal transition (EMT) in tumors and

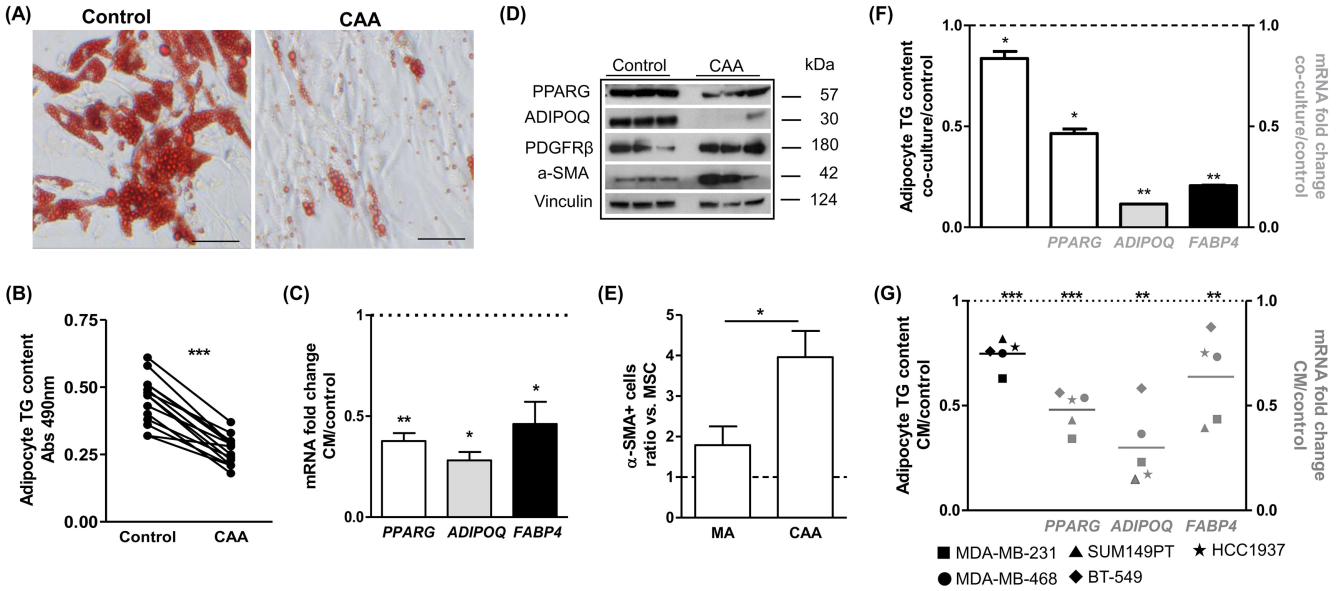

FIGURE 1 TNBC cells induce human ASC52 adipocyte dedifferentiation. (A) Representative Oil Red O-stained lipid droplets in human ASC52 adipocytes cultured for 7 days with conditioned media (CM) from MDA-MB-231 cells or RPMI (Control). Scale bar: 50 µm. (B) Adipocyte triglyceride (TG) content, as measured by Oil Red O staining in adipocytes, treated as described in A. The scatter plot shows the results of independent experiments. ***$p < .001$, by paired Student's *t*-test. (C) Expression levels of common adipocyte genes (*PPARG*, *ADIPOQ*, and *FABP4*) in adipocytes, treated as described in A, as evaluated by qRT-PCR. *B2M* was used as a housekeeping gene. Data (mean ± SEM of 4 independent experiments) are reported as fold-change relative to the expression level in control cells (dotted line). *$p < .05$, **$p < .01$ by paired Student's *t*-test. (D) Western blot analysis of adipocyte markers (PPARG and adiponectin, ADIPOQ) and fibroblast markers (PDGFRβ and α-SMA) in cells treated as described in A. Independent experiments for each condition are shown. Vinculin was used as a loading control. (E) α-SMA positive cells in mature adipocytes (MAs) and MDA-MB-231 modified adipocytes (CAAs), as evaluated by flow cytometry. Data are reported relative to positive cells in ASC52 mesenchymal cells (MSCs) and presented as the mean ± SEM of 4 independent experiments. *$p < .05$ by paired Student's *t*-test (F) Adipocyte TG content (left axis, first bar), as measured by Oil Red O staining, and expression level of adipocyte genes (right axis, gray gene symbol) in adipocytes on co-culture with MDA-MB-231 cells. *$p < .05$, **$p < .01$ by unpaired Student's *t*-test (G), Adipocyte TG contents (left axis, black symbols), as measured by Oil Red O staining, and expression levels of adipocyte genes (right axis, gray symbols) in adipocytes, treated as described in A with CM from various TNBC cell lines. Each symbol represents a cell line (MDA-MB-231, SUM149PT, MDA-MB-468, BT549, HCC1937) and is presented as the mean of at least 3 independent experiments. Data are reported relative to control (dotted line, adipocytes treated with RPMI). *$p < .05$, **$p < .01$, ***$p < .001$ by paired Student's *t*-test.

cancer stem cell (CSC) enrichment,[30,31] which are associated with tumor aggressiveness and metastasis,[32] we measured the expression of select genes that are related to lipid metabolism, EMT, and CSC phenotype. Fatty acid synthase (*FASN*), the sole mammalian enzyme that catalyzes de novo fatty acid synthesis, was significantly reduced in MDA-MB-231 cells that were exposed to CAA CM (Supplementary Figure S2B); although fatty acid transporter protein 2 (FATP2, *SLC27A2*) was not modulated by CM, the intracellular lipid chaperone fatty acid-binding protein 4 (*FABP4*), was significantly upregulated only in BC cells that were exposed to CAA CM (Supplementary Figure S2B).

MAs and CAAs had similar effects on inducing the EMT phenotype in MDA-MB-231 cells, compared with ASC52 MSCs. In MDA-MB-231 cells that were treated with MA and CAA CM, E-cadherin (*CDH1*) expression fell significantly, and SNAIL2 (*SNAI2*), fibronectin (*FN1*), and TGFβ receptor (*TGFBR2*) were upregulated, compared with controls (Supplementary Figure S2C). Conversely, only CAAs had a prominent impact on the CSC-like phenotype in MDA-MB-231 cells, as evidenced by significantly higher levels of *NANOG* and *OCT4* transcripts versus the other conditions (control, MSC, and MA; Supplementary Figure S2D).

3.3 | Cancer-associated adipocytes influence the tumor immune microenvironment, inducing neutrophil recruitment

Because our GEP results showed that tumor-induced changes to adipocytes were associated primarily with inflammation and immune cell chemotaxis, we evaluated leukocyte recruitment due to MA and CAA CM by chemotaxis assay. MA and CAA CM recruited more leukocytes in general—specifically, granulocytes—than control media (Supplementary Figure S3A), more so with CAA CM than MA CM ($p = .0395$, $p = .0379$, respectively; Figure 3A,B). Accordingly, in an analysis of migrating cells by multiparametric flow cytometry (Figure 3C–G), there was no significant difference in T cells, B cells, monocytes, or natural killer cells (Figure 3D–G), whereas neutrophils were more strongly attracted by CAA CM than

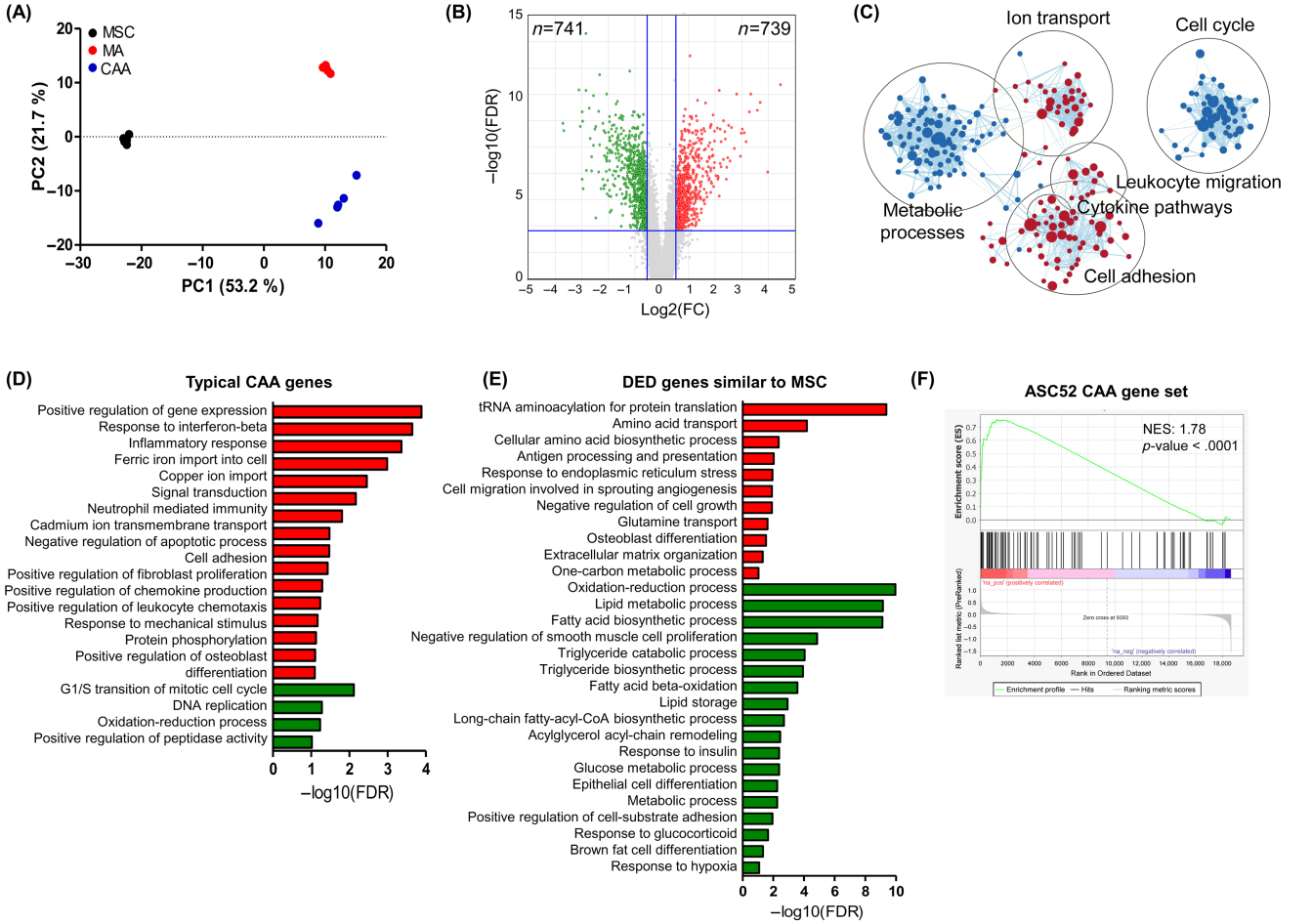

FIGURE 2 Molecules released by MDA-MB-231 cells induce a specific gene expression profile in ASC52 adipocytes. (A) Principal component analysis (PCA) score plot, based on the gene expression profile of ASC52 mesenchymal cells (MSC), mature adipocytes cultured in RPMI (MA), or adipocytes modified by the conditioned medium from MDA-MB-231 cells (CAA). Each dot represents an independent biological replicate. (B) Volcano plot of $\log_2$ fold-change (FC) versus $-\log_{10}$ false discovery rate (FDR), showing transcriptional differences between ASC52 CAA and MA cells. Vertical blue lines represent the cutoff of a change of 1.5, and the horizontal blue line denotes the 0.1-FDR cut-off. Upregulated and downregulated genes are highlighted in red and green, respectively. (C) Enrichment map showing significantly enriched GO terms (Gene Ontology Biological Processes, FDR < .1) related to differences in the transcriptomes of ASC52 CAA and MA cells. Hypergeometric tests of GO terms were performed using GSEA. The color of the node shows positive (red) and negative (blue) enrichment of GO terms in CAA cells. Circles show summarized GO term clusters, based on Auto Annotate. Enrichment maps were created using the Cytoscape Enrichment Map plugin. (D and E) GO terms (Gene Ontology Biological Processes) significantly (FDR < .1) overrepresented in upregulated (red) and downregulated (green) (FDR < .1) genes that were shared between the comparisons CAA versus MA and CAA versus MSC (typical CAA genes, $n = 543$) (D) and those shared between the comparisons MSC versus MA and MA versus CAA, with the opposite expression (E). (F) GSEA enrichment plots of the ASC52 CAA gene set, consisting of genes typical of CAA (FC >2, FDR <0.1, $n = 95$) in tumor-adjacent AT compared with matched tumor-distant AT, from patients with BC. NES, normalized enrichment score.

MA CM ($p = .0200$, Figure 3C and Supplementary Figure S3B,C). CAA CM contained significantly higher levels of well-known neutrophil chemotactic factors, such as CXCL5 and IL-8 (CXCL8) than CM from MA (CXCL5, $p = .0579$; IL-8, $p = .0166$) and MSC (CXCL5, $p = .0028$; IL-8, $p = .0390$) (Figure 3H,I). Moreover, the combination of neutralizing antibodies against IL-8 and CXCL5 significantly impeded the CAA CM-induced recruitment of leukocytes and granulocytes ($p = .0100$, $p = .0372$, respectively; Figure 3J).

Similar results were obtained in murine 3T3-L1 CAAs that were induced by murine 4T1 TNBC cells, (Supplementary Figure S4). CAA CM effected greater splenocyte recruitment than MA CM ($p = .0032$, Supplementary Figure S5A), although the greater recruitment of the myeloid component by CAAs in this model, especially granulocytes, was accompanied by increased attraction of T lymphocytes, NKs, and monocytes, compared with MAs (Supplementary Figure S5B,C). By Bioplex analysis of 3T3-L1 CM, CAAs released significantly more IL-6, CCL2, CXCL5, and chemokines (CXCL1, CXCL10, CXCL12, and CCL7) versus MAs (Supplementary Figure S5D), supporting the increased immune cell recruitment by CAAs.

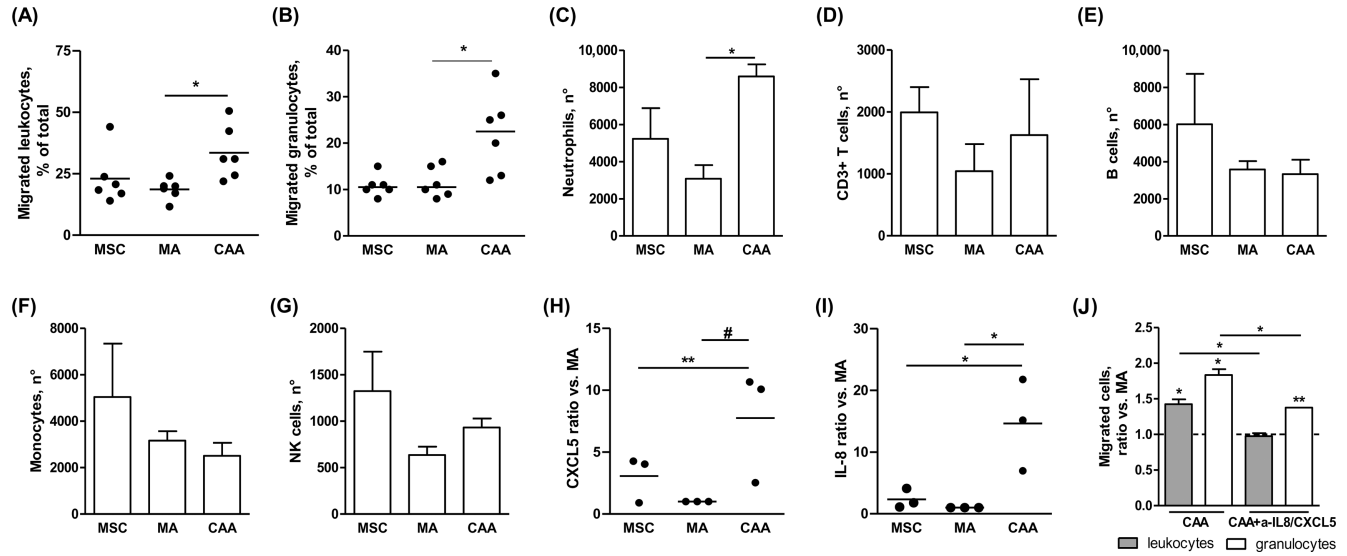

FIGURE 3 ASC52 cancer-associated adipocytes recruit neutrophils. (A-B) Percentage of leukocytes (A) and granulocytes (B) that migrated toward CM derived from ASC52 mesenchymal cells (MSC), mature adipocytes (MA), and tumor-modified adipocytes (CAA), during a 6 h migration assay. Results are reported as the percentage of total leukocytes seeded in the Boyden chamber. Each dot represents the mean of 2 technical replicates of independent experiments. (C-G) Number of migrated neutrophils ($CD3^-CD15^+CD14^-CD16^+$, C), T cells ($CD3^+$, D), B cells ($CD3^-CD19^+$, E), monocytes ($CD3^-CD14^+$, F) and NK cells ($CD3^-CD16^+CD56^+$, G), as evaluated by flow cytometry. Data are presented as the mean ± SEM of 3 independent experiments. (H–I) ELISA-based quantification of CXCL5 (H) and IL-8 (I) in ASC52 MSC, MA, and CAA CM. $^{\#}p < .1$, $^{*}p < .05$, $^{**}p < .01$ by paired Student's *t*-test. (J) Leukocytes and granulocytes that migrated toward CAA CM in the presence or absence of antibodies against IL-8 and CXCL5, in a 6 h migration assay. Data are reported relative to cells that migrated toward MA CM (dotted line) and are presented as the mean ± SD of 3 independent experiments. $^{*}p < .05$, $^{**}p < .01$ by unpaired Student's *t*-test.

3.4 | SAA1 is the tumor-derived molecule that regulates adipocyte reprogramming in TNBC cells

To identify the molecules that mediate tumor-driven adipocyte reprogramming, we first examined the biochemistry and secretory mechanisms of BC-derived molecules that induce adipocyte dedifferentiation. By performing vesicle depletion (Supplementary Figure S6A,D), protein denaturation, lipid depletion (Supplementary Figure S6B,E), and size fractionation (Supplementary Figure S6C) in CM, we found that the relevant molecules were free proteins and or lipids with a molecular weight between 10 and 50 kDa.

By liquid chromatography (LC)-tandem mass spectrometry (MS/MS) of a 10–20-kDa band that differentiated the proteinograms of MDA-MB-231 and MDA-MB-361 cells (Supplementary Figure S6F), the latter of which were unable to induce adipocyte dedifferentiation (Supplementary Figure S6G), we identified SAA1 (22% sequence coverage, 1 peptide), cystatin S (75.18% sequence coverage, 4 peptides), cystatin C (57.53% sequence coverage, 10 peptides), cystatin SN (65.96% sequence coverage, 7 peptides), and S100A6 (28.07% sequence coverage, 3 unique peptides). By western blot of these molecules, SAA1 was the only molecule that exclusive to MDA-MB-231 CM (Supplementary Figure S6H), and its release from MDA-MB-231 cells was confirmed by ELISA analysis (Figure 4A). Among the CM of several BC, SAA1 was present only in CM from TNBC cell lines (MDA-MB-231, SUM159PT, SUM149PT, MDA-MB-468, BT-549) versus other BC cells (T47D, MCF7, MDA-MB-361, BT-474, ZR-75-30, HCC1954, SK-BR-3, Figure 4A), implicating SAA1 as a leading causative factor in TNBC cell-adipocyte crosstalk.

Notably, indirect co-culture of MDA-MB-231 cells with adipocytes or MA and CAA CM significantly increased tumoral SAA1 expression (Supplementary Figure S7A,B). This upregulation was independent of SAA1 basal expression in tumor cells, because treatment of SUM149PT cells with MA and CAA CM induced a 3-fold increase in SAA1 expression, as in MDA-MB-231 cells (Supplementary Figure S7C).

To determine the direct involvement of TNBC-released SAA1 during adipocyte reprogramming, siRNA-mediated knockdown of SAA1 was performed in MDA-MB-231 and SUM149PT TNBC cells using 2 independent siRNAs. Adipocytes that were treated with CM from SAA1-1 knockdown cells, which released significantly less SAA1 than control cells (Figure 4B,C) had significantly a higher triglyceride content (Figure 4E,F) and did not undergo the morphological transition to fibroblast-like spindle cells, as observed in adipocytes that were treated with control CM (derived from cells that had been transfected with scramble siRNA, Figure 4D). Accordingly, compared with the control, cells that were grown with CM from SAA1-silenced tumor cells upregulated the differentiation markers *PPARG*, *ADIPOQ*, *FABP4* and *CD36* (Figure 4G,H). In addition, the expression of inflammatory genes decreased significantly, such as *IL6* and *P2X7R*, (Figure 4G,H), which were among the most significantly upmodulated genes in CAAs versus MAs (FDR <0.0001). The 2 SAA1-specific siRNAs significantly reduced SAA1 levels in MDA-MB-468 cells, which released significantly lower basal levels of SAA1 than other 2 TNBC cell lines that we analyzed

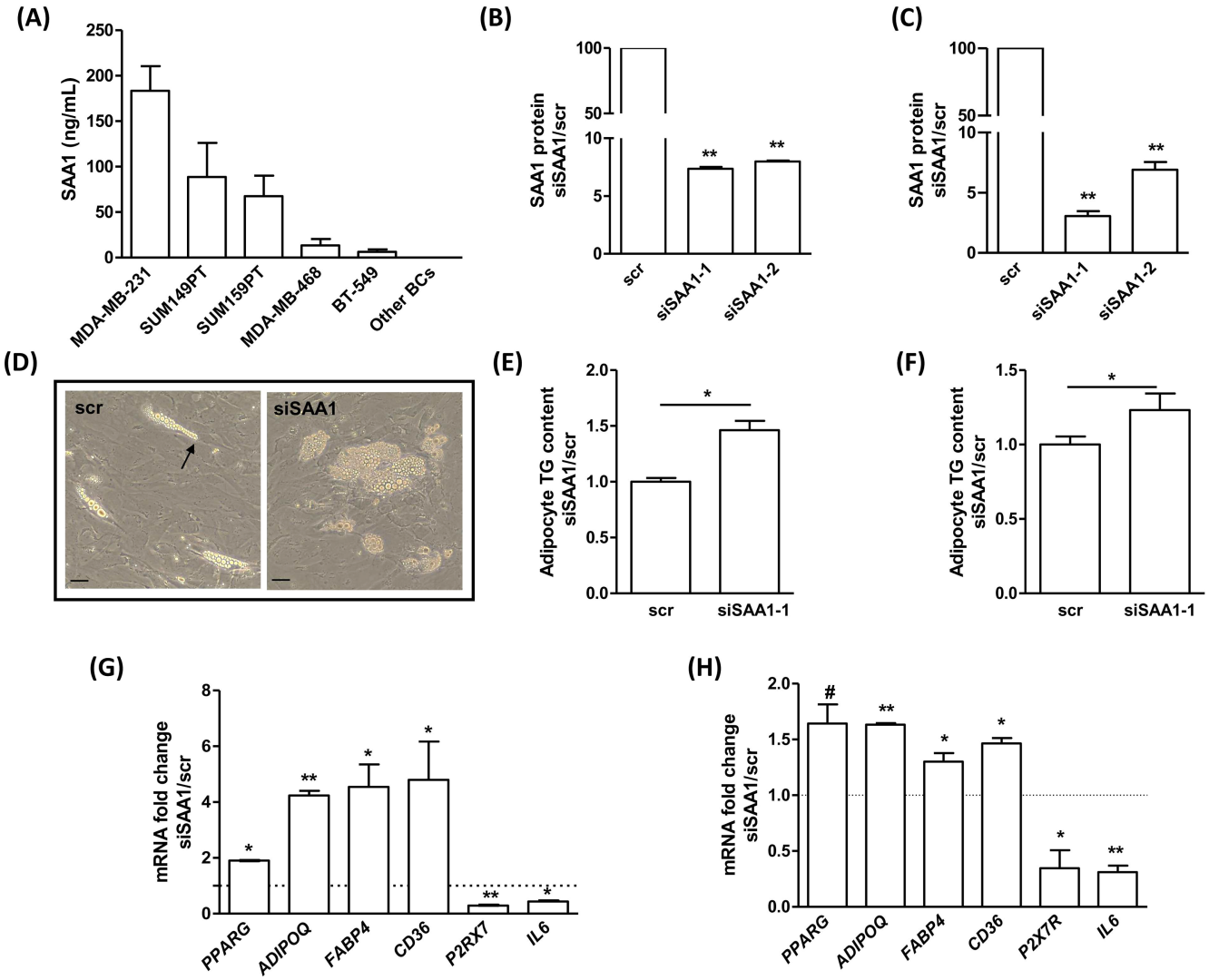

FIGURE 4 SAA1 is causally involved in adipocyte reprogramming in TNBC cells. (A) SAA1 contents in CM derived from TNBC and other BC cell lines (T47D, MCF7, MDA-MB-361, BT-474, ZR-75-30, HCC1954, SK-BR-3). SAA1 was detectable only in TNBC. (B and C) SAA1 content in CM of MDA-MB-231 (B) and SUM149PT (C) cells treated with 2 SAA1 siRNAs (siSAA1-1, siSAA1-2) compared with those treated with scramble siRNA (scr). (D) Representative image of ASC52 adipocytes treated with CM from siSAA1-1-treated or scramble siRNA (scr)-treated MDA-MB-231 cells. Scale bars: 50 µm. (E–H) Adipocyte triglyceride (TG) content, as measured by Oil Red O staining, and relative expression of adipocyte and inflammatory genes, as analyzed by qRT-PCR (G and H) in ASC52 adipocytes treated for 7 days with CM from siSAA1-1-treated or scramble siRNA (scr)-treated MDA-MB-231 (E and G) and SUM149PT (F and H) cells. *B2M* was used as a housekeeping gene. All data are presented as the mean ± SD and are representative of 3 independent experiments. $^{\#}p < .1$, $^{*}p < .05$, $^{**}p < .01$, by unpaired Student's *t*-test.

(Figure 4A), but no consistent effect in inhibiting CM-induced adipocyte modifications was observed (data not shown), supporting a dose-dependent effect on SAA1-mediated induction of CAAs.

3.5 | The CD36 and P2X7R receptors, NF-κβ, and JNK are involved in SAA1-mediated adipocyte reprogramming

To determine the pathways that are modulated during SAA1-dependent induction of adipocyte reprogramming, we administered inhibitors of SAA1 receptors (P2X7R, CD36, TLRs).[33–35] *PPARG* reduction in adipocytes that was induced by MDA-MB-231 CM or human recombinant SAA1 was reverted by a P2X7R inhibitor and by hexarelin (Figure 5A,B), which binds to CD36 in the SAA1-binding site (Asn^{132}-Met^{169}) and inhibits CD36-dependent SAA1 activity in HEK293 cells and macrophages.[35] On the contrary, the CD36 inhibitor SSO and TLR2- and TLR4-blocking antibodies did not impact the reduction in *PPARG* in CAAs (Supplementary Figure S8A and Figure 5A,B, respectively). To examine downstream events, we analyzed the phosphorylation of signal transducers of the P2X7R and CD36 receptors in MAs and in adipocytes on treatment with CM that was derived from SAA1-silenced and control MDA-MB-231 cells by western blot (Figure 5C and Supplementary Figure S8B). Although we

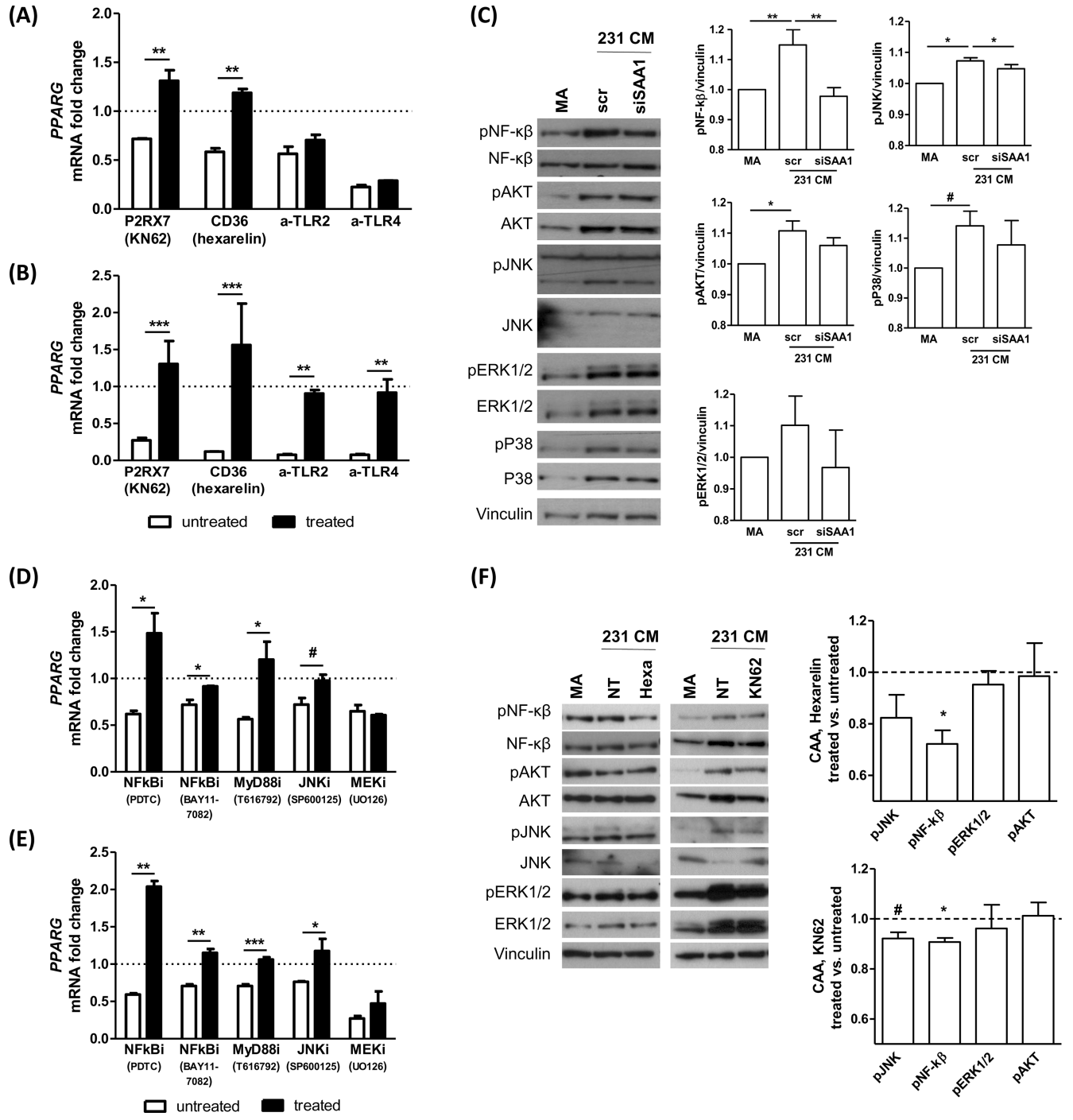

FIGURE 5 CD36 and P2XR7 receptors are involved in SAA1-mediated adipocyte reprogramming. (A and B) Relative *PPARG* expression levels in ASC52 adipocytes cultured with MDA-MB-231 CM (A) or recombinant human SAA1 (B) and treated or not with inhibitors of SAA1 receptors compared with control (adipocytes cultured with RPMI, dotted line). *B2M* was used as a housekeeping gene. Data are presented as the mean ± SD and are representative of 3 independent experiments. $^{**}p < .01$, $^{***}p < .001$, by unpaired Student's *t*-test. (C) Western blot analysis of ASC52 adipocytes cultured for 48 h with control medium (RPMI, MA) or CM from MDA-MB-231 cells upon transfection with SAA1 siRNA (siSAA1) or scramble siRNA (scr). Vinculin was used as a loading control. Data are representative of 4 independent experiments. Densitometric quantification of the phospho-proteins versus vinculin is shown on the right. Data are presented as the mean ± SEM of 4 independent experiments. $^{\#}p < .1$, $^{*}p < .05$, $^{**}p < .01$, by paired Student's *t*-test. (D and E) Relative *PPARG* expression levels in ASC52 adipocytes cultured with MDA-MB-231 CM (D) or recombinant human SAA1 (E) and treated or not with inhibitors of SAA1 receptor downstream signals compared with controls (adipocytes cultured with control RPMI, dotted line). *B2M* was used as a housekeeping gene. Data are presented as the mean ± SD and are representative of 3 independent experiments. $^{\#}p < .1$, $^{*}p < .05$, $^{**}p < .01$ $^{***}p < .001$, by unpaired Student's *t*-test. (F) Western blot analysis of ASC52 adipocytes cultured for 48 h with control medium (RPMI, MA) or MDA-MB-231 CM in the presence or absence (NT) of hexarelin (Hexa) or KN62. Vinculin was used as a loading control. Data are representative of 4 independent experiments. Densitometric quantification of the phospho-proteins versus vinculin is shown on the right. Data are presented as the mean ± SEM of 4 independent experiments. $^{\#}p < .1$, $^{*}p < .05$, by paired Student's *t*-test.

observed a significant increase in the total amount of phospho-NF-κβ, -JNK and -AKT in adipocytes during reprogramming versus MAs, only NF-κβ and JNK phosphorylation were significantly lower in adipocytes that had been cultured with CM from SAA1-silenced tumor cells compared with control (Figure 5C). Of note, a SAA1-dependent increase in the phosphorylated protein levels, compared to the total protein amount, was observed in the NF-κβ pathway (trend *p*-value), along with a noticeable trend in the JNK pathway (Supplementary Figure S8B). Accordingly, the NF-κβ inhibitors PDTC and BAY11-7082 and the JNK inhibitor SP600125 significantly blocked the reduction in *PPARG* expression that was induced by MDA-MB-231 CM or recombinant SAA1 (Figure 5D,E). Similar results were obtained with the MyD88 inhibitor T616792, which acts as a P2X7R adaptor protein in NF-κβ activation,[36] whereas the ERK1/2 inhibitor UO126 did not affect *PPARG* expression in adipocytes.

NF-κβ and JNK phosphorylation were inhibited in adipocytes on culture with MDA-MB-231 CM in the presence of hexarelin or the P2X7R inhibitor KN62 (Figure 5F and Supplementary Figure S8C),

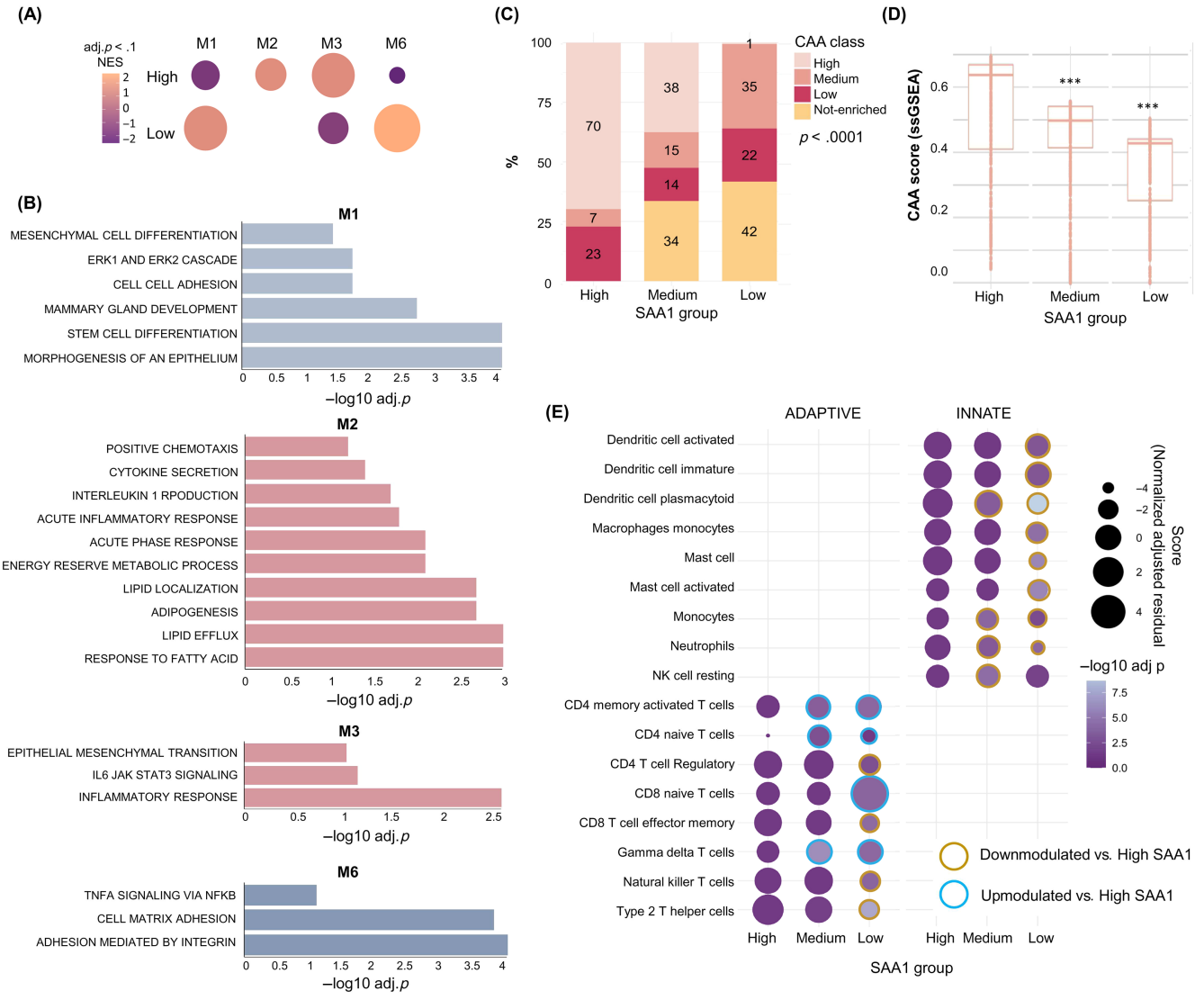

FIGURE 6 SAA1 expression is associated with aggressive features in human TNBCs. (A) Gene Set Enrichment Analysis of significantly enriched co-expression modules among tumors with high and low SAA1 mRNA expression. NES, normalized enrichment score. The size and color of the circle represent the normalized enrichment score (NES). (B) Over-representation analysis of significant modules using gene sets from the Cancer hallmarks and Gene Ontology terms from the Msigdb database. Bar graph shows the log 10-adjusted *p*-value of the enrichment between genes in modules and gene sets from the Reactome Pathway database. The pathways were ordered by significance as indicated on the x-axis. (C) Frequency of CAA class (high, medium, low), as evaluated by ssGSEA in each SAA1 tumor group (high, medium, low). Negative ssGSEA values were considered as not-being enriched. *p*-value by chi-square test. (D) ssGSEA CAA score in TNBCs according to SAA1 expression (high, medium, low). ***$p < .001$ by *t*-test. (E) Bubble plot shows the comparison of significant differentially enriched (adjusted BH *p*-value <.1) infiltrating immune cells in each SAA1 tumor group (high, medium, and low), computed by CIBERSORTx, Xcell or ssGSEA of public signatures. Bubble size represents tumor purity-adjusted immune scores, whereas color denotes the probability value. Outer circle indicates whether the immune term is downmodulated (gold) or upregulated (blue) against SAA1-high tumors.

confirming the relevance of these signals in SAA1-mediated adipocyte reprogramming. These pharmacological and genetic studies support the involvement of P2XR7, CD36, JNK, and NF-κβ in the SAA1-mediated adipocyte reprogramming.

3.6 | SAA1 is associated with aggressiveness in TNBC

To examine the clinical impact of SAA1-dependent tumor-adipocyte interaction, a cohort of 1311 TNBCs was analyzed by SAA1 expression. Co-Expression Molecules identification Tool (CEMiTool) identified 6 coexpression modules (Supplementary Table S3), of which modules M1, M2, M3, and M6 were significantly and differentially enriched in tumors that overexpressed SAA1 (SAA1-high) versus SAA1-low tumors (Figure 6A and Supplementary Table S3). Modules M2 and M3 were positively enriched, whereas M1 and M6 were negatively enriched in SAA1-high tumors. Similar to our in vitro results, module M2 contained genes that were related to inflammation, chemotaxis, lipid efflux, and lipolysis, and M3 harbored genes that are involved in EMT and inflammation (Figure 6B and Supplementary Table S3). SAA1-high tumors also downmodulated differentiation pathways of stem and mesenchymal cells, which were enriched in M1 (Figure 6B and Supplementary Table S3). Notably, *SAA1* was identified as a relevant hub of module M2 with genes that are linked to inflammation, angiogenesis, cell cycle progression, and lipid metabolism (Supplementary Figure S9).

Consistent with our in vitro data on the relevance of SAA1 to adipocyte reprogramming, CAA scores, which are based on the expression of 22 genes that were upmodulated in tumor-adjacent versus tumor-distant AT (see Section 2.9), were higher in SAA1-high than SAA1-low tumors (Figure 6C,D). Further, in support of the CAA induction of tumor stem-like properties and immune cell chemotaxis, SAA1 mRNA expression was significantly upregulated in TNBCs that have been categorized as mesenchymal stem-like (MSL) per the Lehmann classification[2] compared with other subtypes (Supplementary Figure S10A). In addition, SAA1-high tumors had lower differentiation scores,[27] which closely resembles the differentiation dynamics of mammary epithelial stem cells, than SAA1-low tumors (Supplementary Figure S10B). SAA1-high tumors experienced significantly greater infiltration by neutrophils, monocytes, and dendritic cells and less infiltration by CD4 and gamma delta T-cells than SAA1-medium and SAA1-low tumors (Figure 6E and Supplementary Table S4).

Overall, these data demonstrated that high SAA1 mRNA expression in human TNBCs correlates with the presence of CAAs and aggressive features that we have shown to be regulated by CAAs in TNBC cells in vitro, supporting the importance of tumor-released SAA1 in mediating tumor-adipocyte crosstalk.

4 | DISCUSSION

When human BC cells break through the basal membrane, they remain in close contact with adipocytes. Thus, the intimate crosstalk between these 2 cell types, which has been described in vitro and in vivo,[8,11] is likely to be relevant to cancer progression. In the current study, we identified a tumor-derived molecule, SAA1, as the molecular crux of the crosstalk between TNBCs and human adipocytes.

ASC52 adipocytes had a unique gene expression profile that was driven by cancer cells and detectable in patient-derived tumor-adjacent AT compared with tumor-distant AT, indicating that the in vitro cellular model that we used resembles human adipose tissue. The CAA-unique features were related primarily to inflammation, as several CAA-specific genes belong to the inflammatory response process and several DEGs in the comparison between CAAs and MAs are target genes of proinflammatory molecules (TNF, ATF4, IL6, IFNG, IL1B and NF-κβ; Supplementary Table S5).

CAA-related inflammation is likely to be amplified by neutrophils, which are highly recruited by CAAs through the production of CXCL5 and IL-8, as we demonstrated in vitro. Neutrophil recruitment appears to be the primary event in the initiation of the inflammatory cascade in adipose tissue during metabolic disorders[37] and mediates the development of AT inflammation.[38] In addition, neutrophils have potential relevance to tumor progression, because emerging evidence suggests that neutrophils are active factors in cancer progression[39] and in the suppression of the antitumor immune response.[40] Thus, it is conceivable that tumor-adipocyte crosstalk modifies the inflammatory status of the tumor microenvironment, inducing tumor progression. In support of this model, SAA1-overexpressing TNBCs experienced greater infiltration by neutrophils and other pro-tumor immune cells than SAA1-low tumors.

In conjunction with the unique inflammatory state of CAAs, we speculate that the metabolic phenotype of CAAs that was predicted by our gene expression analysis (i.e., increased glutamine release and amino acid biosynthesis and release) is relevant in the malicious crosstalk with tumor cells. Glutamine provides a survival advantage to TNBC cells that are dependent on extracellular glutamine[41] and amino acids potentiate cancer cell invasiveness and stemness.[42] Moreover, lipids that are released by adipocytes during dedifferentiation can be scavenged by cancer cells, as demonstrated in breast, prostate and ovarian cancer,[43–45] sustaining cancer progression.[46,47] This metabolic crosstalk between BC cells and adipocytes is supported by the upmodulation of the lipid chaperone FABP4 and the downregulation of fatty acid synthase we observed in MDA-MB-231 cells on culture with CAA CM. Notably, chaperone expression was recently demonstrated to be critical for TNBC and ovarian cancer metastasis.[48–50] Our findings provide evidence for the existence of heterogeneity in the crosstalk between BC cells and adipocytes. This conclusion is drawn from the described increase in molecules associated with lipid internalization in TNBC cells (e.g., MDA-MB-468), when subjected to indirect co-culture with mature adipocytes through the use of CM,[45] with this induction being unique to CAAs in our study in the case of MDA-MB-231 cells.

We identified SAA1, a small apolipoprotein, as an important molecule that is released by TNBC cells, to reprogram adipocytes. SAA1 has various functions, and was recently proposed as a cancer biomarker, based on its high expression in the blood of cancer patients

and its expression in cancer tissues.[21] However, its direct involvement in cancer biology is just emerging,[16–18,20,51] and our data contribute to our knowledge of its function in cancer progression, primarily as modulator of the tumor microenvironment. The high heterogeneity of SAA1 expression we observed in human TNBCs and its positive association with CAA score other than the features that are regulated by CAAs in vitro (i.e., CSC properties, FA uptake, inflammation and immune cell recruitment) suggests that the heterogeneity of TNBC disease[2,3] also applies to adipocyte reprogramming. Thus, tumor cells that express high levels of SAA1 are more likely to interact with and subvert cells in the tumor microenvironment to progress.

SAA1 was released exclusively by TNBC cells, as observed in patients,[18] indicating that the mechanisms of CAA induction differ between BC subtypes. Several molecules might be necessary to trigger this process, and each BC subtype might express a specific molecule that converges on the same signaling pathway toward adipocyte reprogramming. The identification of candidate tumor-derived molecules, such as TNFα, Wnt3a, and Wnt5a in regulating adipocyte dedifferentiation,[12] supports this model. Even among TNBC cells, the SAA1-mediated changes to adipocytes are relevant only in highly expressing cells. Interestingly, SAA1 expression in tumor cells was boosted both by CAAs, as described in pancreatic tumors,[52] but also by MA CM, speculating that host adipocytes may start their crosstalk with tumor cells.

In addition, because we found that SAA1 silencing in tumor cells modulates adipocyte dedifferentiation, delipidation and inflammation, it is likely that these characteristics are interconnected in the process of adipocyte reprogramming and are not independent properties that are influenced by different molecules. The activity of P2X7R and CD36 receptors in modulating the inflammatory response and the lipid metabolism in various cell lines and in adipocytes from patients with metabolic disorders[35,53,54] supports this hypothesis.

The activity of tumor-derived SAA1 engages the P2X7R and CD36 receptors on adipocytes and the downstream molecules NF-κβ and JNK. Indeed, within TNBC CM, the presence of SAA1 significantly increased the phosphorylation levels of these molecules, triggering an amplification of these pathways, possibly driven by an increase in both transcription/translation and phosphorylation processes. Interestingly, SSO, a compound commonly used to inhibit CD36-dependent FA uptake by binding to the CD36 lysine 164 residue,[55] unlike hexarelin, did not block adipocyte reprogramming induced by TNBC cells. These results suggest that SSO may not inhibit the binding of SAA1 to CD36, warranting further investigation to elucidate the precise mechanisms at play in this context. In addition, our data exclude the involvement of TLR receptors because the TLR-related effects that are induced by recombinant SAA1 likely depend on bacterial contaminants.[56]

Our study has limitations. First, our data are based on results that were obtained with ASC52 cells, which serve as a model of human adipocytes, but might not fully mimic the heterogeneity and phenotype of primary adipocytes. Thus, the relevance of SAA1 and its effects on adipocytes warrant validation in other models. Furthermore, the use of tumor medium conditioned for 72 h, which may be devoid of essential growth factors, in the majority of our experiments, although it does not preclude us from assessing the relevance of SAA1 in the interaction between TNBC cells and adipocytes, might have influenced our results. Moreover, further research is required to confirm the molecular mechanisms involved in adipocyte reprogramming and the direct roles of CD36 and P2X7R receptors and downstream signals in the communication between tumor cells and adipocytes.

In conclusion, adipocyte reprogramming is controlled by SAA1 in TNBC cells. Although the direct regulation of protumoral features by SAA1 in tumor cells cannot be excluded,[18,20] our data strongly support that they are governed by SAA1-mediated crosstalk between tumor cells and adipocytes.

AUTHOR CONTRIBUTIONS

TT and IR conceived the study; IR, NM, SLRC, VR, VC, LdC, EM, and FB carried out experimental procedures; TT, IR, NM, SLRC, LdC, EM, BP, FB, LS, and GT performed formal analysis and investigation; RA acquired resources; TT, IR, and SLRC wrote the manuscript; TT and ET supervised the study. All authors approved the final version of the manuscript. The work reported in the paper has been performed by the authors, unless clearly specified in the text.

ACKNOWLEDGMENTS

We thank Mrs. Ghirelli for technical assistance, the Functional Genomics Core Facility and the Flow Cytometry and Cell Sorting Facility of Fondazione IRCCS Istituto Nazionale dei Tumori, Milan for their support in performing the gene expression profile analyses and multiparametric cytofluorimetric analyses, respectively. We thank Mrs. Mameli for secretarial assistance. We thank Blue Pencil Science (http://www.bluepencilscience.com/) for editing an English draft of this manuscript. Open access funding provided by BIBLIOSAN.

FUNDING INFORMATION

The research leading to these results has received funding from Fondazione AIRC under IG 2016—ID 18712 project; IG 2020—ID 24984 project—P.I. Triulzi Tiziana and from AIRC and Fondazione Cariplo under TRIDEO 2014—ID 16117—P.I. Triulzi Tiziana. Ilona Rybinska was supported by a Fondazione Umberto Veronesi fellowship. This research was partially supported by Italian Ministry of Health "Ricerca Corrente" funds.

CONFLICT OF INTEREST STATEMENT

The authors declare no conflicts of interest.

DATA AVAILABILITY STATEMENT

Data sources and handling of the publicly available datasets used in this study are described in Section 2. The raw gene expression profiling data generated in this study is available in GEO under accession number GSE153316 and GSE153317. The raw mass spectrometry data generated in this study have been submitted to PRIDE under dataset identifier PXD041186. Other data that support the findings

of this study are available from the corresponding author upon request.

ETHICS STATEMENT

The research protocol for this study was approved by the Independent Ethics Committee of Fondazione IRCCS Istituto Nazionale dei Tumori. Informed consent from all the participants in this study was obtained.

ORCID

Loris De Cecco https://orcid.org/0000-0002-7066-473X
Tiziana Triulzi https://orcid.org/0000-0003-3050-8676

TWITTER

Tiziana Triulzi *TizianaTriulzi*

REFERENCES

1. Siegel RL, Miller KD, Fuchs HE, Jemal A. Cancer statistics, 2022. *CA Cancer J Clin*. 2022;72:7-33.
2. Lehmann BD, Bauer JA, Chen X, et al. Identification of human triple-negative breast cancer subtypes and preclinical models for selection of targeted therapies. *J Clin Invest*. 2011;121:2750-2767.
3. Loi S, Michiels S, Adams S, et al. The journey of tumor-infiltrating lymphocytes as a biomarker in breast cancer: clinical utility in an era of checkpoint inhibition. *Ann Oncol*. 2021;32:1236-1244.
4. Yam C, Mani SA, Moulder SL. Targeting the molecular subtypes of triple negative breast cancer: understanding the diversity to progress the field. *Oncologist*. 2017;22:1086-1093.
5. Rybinska I, Agresti R, Trapani A, Tagliabue E, Triulzi T. Adipocytes in breast cancer, the thick and the thin. *Cell*. 2020;9:9.
6. Hardaway AL, Herroon MK, Rajagurubandara E, Podgorski I. Bone marrow fat: linking adipocyte-induced inflammation with skeletal metastases. *Cancer Metastasis Rev*. 2014;33:527-543.
7. Corsa CAS, MacDougald OA. Cyclical dedifferentiation and redifferentiation of mammary adipocytes. *Cell Metab*. 2018;28:187-189.
8. Tan J, Buache E, Chenard MP, Dali-Youcef N, Rio MC. Adipocyte is a non-trivial, dynamic partner of breast cancer cells. *Int J Dev Biol*. 2011;55:851-859.
9. Duong MN, Geneste A, Fallone F, Li X, Dumontet C, Muller C. The fat and the bad: mature adipocytes, key actors in tumor progression and resistance. *Oncotarget*. 2017;8:57622-57641.
10. Dirat B, Bochet L, Dabek M, et al. Cancer-associated adipocytes exhibit an activated phenotype and contribute to breast cancer invasion. *Cancer Res*. 2011;71:2455-2465.
11. Zhu Q, Zhu Y, Hepler C, et al. Adipocyte mesenchymal transition contributes to mammary tumor progression. *Cell Rep*. 2022;40:111362.
12. Rybinska I, Mangano N, Tagliabue E, Triulzi T. Cancer-associated adipocytes in breast cancer: causes and consequences. *Int J Mol Sci*. 2021;22:3775.
13. Urieli-Shoval S, Cohen P, Eisenberg S, Matzner Y. Widespread expression of serum amyloida A in histologically normal human tissues: predominant localization to the epithelium. *J Histochem Cytochem*. 1998;46:1377-1384.
14. Yang M, Liu F, Higuchi K, et al. Serum amyloid A expression in the breast cancer tissue is associated with poor prognosis. *Oncotarget*. 2016;7:35843-35852.
15. Zhou J, Sheng J, Fan Y, et al. Association between serum amyloid A levels and cancers: a systematic review and meta-analysis. *Postgrad Med J*. 2018;94:499-507.
16. Hansen MT, Forst B, Cremers N, et al. A link between inflammation and metastasis: serum amyloid A1 and A3 induce metastasis, and are targets of metastasis-inducing S100A4. *Oncogene*. 2015;34:424-435.
17. Olivier DW, Pretorius E, Engelbrecht A-M. Serum amyloid A1: innocent bystander or active participant in cell migration in triple-negative breast cancer? *Exp Cell Res*. 2021;406:112759.
18. Ignacio RMC, Gibbs CR, Kim S, Lee ES, Adunyah SE, Son DS. Serum amyloid A predisposes inflammatory tumor microenvironment in triple negative breast cancer. *Oncotarget*. 2019;10:511-526.
19. Li Z, Hou Y, Zhao M, et al. Serum amyloid A, a potential biomarker both in serum and tissue, correlates with ovarian cancer progression. *J Ovarian Res*. 2020;13:67.
20. Niu X, Yin L, Yang X, et al. Serum amyloid A 1 induces suppressive neutrophils through the Toll-like receptor 2-mediated signaling pathway to promote progression of breast cancer. *Cancer Sci*. 2022;113:1140-1153.
21. Sack GH. Serum amyloid A (SAA) proteins. *Subcell Biochem*. 2020;94:421-436.
22. Li W, Wang W, Zuo R, et al. Induction of pro-inflammatory genes by serum amyloid A1 in human amnion fibroblasts. *Sci Rep*. 2017;7:693.
23. Triulzi T, Forte L, Regondi V, et al. HER2 signaling regulates the tumor immune microenvironment and trastuzumab efficacy. *Onco Targets Ther*. 2019;8:e1512942.
24. Bianchi F, Sasso M, Turdo F, et al. Fhit nuclear import following EGF stimulation sustains proliferation of breast cancer cells. *J Cell Physiol*. 2015;230:2661-2670.
25. Pereira B, Chin SF, Rueda OM, et al. The somatic mutation profiles of 2,433 breast cancers refines their genomic and transcriptomic landscapes. *Nat Commun*. 2016;7:11479.
26. Yoshihara K, Shahmoradgoli M, Martínez E, et al. Inferring tumour purity and stromal and immune cell admixture from expression data. *Nat Commun*. 2013;4:2612.
27. Prat A, Parker JS, Karginova O, et al. Phenotypic and molecular characterization of the claudin-low intrinsic subtype of breast cancer. *Breast Cancer Res*. 2010;12:R68.
28. Russo PST, Ferreira GR, Cardozo LE, et al. CEMiTool: a Bioconductor package for performing comprehensive modular co-expression analyses. *BMC Bioinform*. 2018;19:56.
29. Charoentong P, Finotello F, Angelova M, et al. Pan-cancer immunogenomic analyses reveal genotype-immunophenotype relationships and predictors of response to checkpoint blockade. *Cell Rep*. 2017;18:248-262.
30. Yi M, Li J, Chen S, et al. Emerging role of lipid metabolism alterations in cancer stem cells. *J Exp Clin Cancer Res*. 2018;37:118.
31. Suarez-Carmona M, Lesage J, Cataldo D, Gilles C. EMT and inflammation: inseparable actors of cancer progression. *Mol Oncol*. 2017;11:805-823.
32. Kong D, Li Y, Wang Z, Sarkar FH. Cancer stem cells and epithelial-to-mesenchymal transition (EMT)-phenotypic cells: are they cousins or twins? *Cancers (Basel)*. 2011;3:716-729.
33. Niemi K, Teirilä L, Lappalainen J, et al. Serum amyloid A activates the NLRP3 inflammasome via P2X7 receptor and a cathepsin B-sensitive pathway. *J Immunol*. 2011;186:6119-6128.
34. Sandri S, Rodriguez D, Gomes E, Monteiro HP, Russo M, Campa A. Is serum amyloid A an endogenous TLR4 agonist? *J Leukoc Biol*. 2008;83:1174-1180.
35. Baranova IN, Bocharov AV, Vishnyakova TG, et al. CD36 is a novel serum amyloid A (SAA) receptor mediating SAA binding and SAA-induced signaling in human and rodent cells. *J Biol Chem*. 2010;285:8492-8506.
36. Liu Y, Xiao Y, Li Z. P2X7 receptor positively regulates MyD88-dependent NF-κB activation. *Cytokine*. 2011;55:229-236.
37. Watanabe Y, Nagai Y, Honda H, et al. Bidirectional crosstalk between neutrophils and adipocytes promotes adipose tissue inflammation. *FASEB J*. 2019;33:11821-11835.
38. Maurizi G, Della Guardia L, Maurizi A, Poloni A. Adipocytes properties and crosstalk with immune system in obesity-related inflammation. *J Cell Physiol*. 2018;233:88-97.

39. Swierczak A, Mouchemore KA, Hamilton JA, Anderson RL. Neutrophils: important contributors to tumor progression and metastasis. *Cancer Metastasis Rev*. 2015;34:735-751.
40. Bronte V, Tortora G. Adipocytes and neutrophils give a helping hand to pancreatic cancers. *Cancer Discov*. 2016;6:821-823.
41. Sun X, Wang M, Wang M, et al. Metabolic reprogramming in triple-negative breast cancer. *Front Oncol*. 2020;10:428.
42. Liao J, Liu PP, Hou G, et al. Regulation of stem-like cancer cells by glutamine through β-catenin pathway mediated by redox signaling. *Mol Cancer*. 2017;16:51.
43. Nieman KM, Kenny HA, Penicka CV, et al. Adipocytes promote ovarian cancer metastasis and provide energy for rapid tumor growth. *Nat Med*. 2011;17:1498-1503.
44. Gazi E, Gardner P, Lockyer NP, Hart CA, Brown MD, Clarke NW. Direct evidence of lipid translocation between adipocytes and prostate cancer cells with imaging FTIR microspectroscopy. *J Lipid Res*. 2007;48:1846-1856.
45. Gyamfi J, Yeo JH, Kwon D, et al. Interaction between CD36 and FABP4 modulates adipocyte-induced fatty acid import and metabolism in breast cancer. *NPJ Breast Cancer*. 2021;7:129.
46. Wang YY, Attané C, Milhas D, et al. Mammary adipocytes stimulate breast cancer invasion through metabolic remodeling of tumor cells. *JCI Insight*. 2017;2:e87489.
47. Zaoui M, Morel M, Ferrand N, et al. Breast-associated adipocytes secretome induce fatty acid uptake and invasiveness in breast cancer cells via CD36 independently of body mass index, menopausal status and mammary density. *Cancers (Basel)*. 2019;11:2012.
48. Mukherjee A, Chiang CY, Daifotis HA, et al. Adipocyte-induced FABP4 expression in ovarian cancer cells promotes metastasis and mediates carboplatin resistance. *Cancer Res*. 2020;80:1748-1761.
49. Apaya MK, Hsiao PW, Yang YC, Shyur LF. Deregulating the CYP2C19/epoxy-eicosatrienoic acid-associated FABP4/FABP5 signaling network as a therapeutic approach for metastatic triple-negative breast cancer. *Cancers (Basel)*. 2020;12:199.
50. Gharpure KM, Pradeep S, Sans M, et al. FABP4 as a key determinant of metastatic potential of ovarian cancer. *Nat Commun*. 2018;9:2923.
51. du Plessis M, Davis TA, Olivier DW, de Villiers WJS, Engelbrecht AM. A functional role for serum amyloid A in the molecular regulation of autophagy in breast cancer. *Front Oncol*. 2022;12:1000925.
52. Takehara M, Sato Y, Kimura T, et al. Cancer-associated adipocytes promote pancreatic cancer progression through SAA1 expression. *Cancer Sci*. 2020;111:2883-2894.
53. Coccurello R, Volonté C. P2X7 receptor in the management of energy homeostasis: implications for obesity, dyslipidemia, and insulin resistance. *Front Endocrinol (Lausanne)*. 2020;11:199.
54. Kennedy DJ, Kuchibhotla S, Westfall KM, Silverstein RL, Morton RE, Febbraio M. A CD36-dependent pathway enhances macrophage and adipose tissue inflammation and impairs insulin signalling. *Cardiovasc Res*. 2011;89:604-613.
55. Kuda O, Pietka TA, Demianova Z, et al. Sulfo-N-succinimidyl oleate (SSO) inhibits fatty acid uptake and signaling for intracellular calcium via binding CD36 lysine 164: SSO also inhibits oxidized low density lipoprotein uptake by macrophages. *J Biol Chem*. 2013;288:15547-15555.
56. Abouelasrar Salama S, de Bondt M, de Buck M, et al. Serum amyloid A1 (SAA1) revisited: restricted leukocyte-activating properties of homogeneous SAA1. *Front Immunol*. 2020;11:843.

SUPPORTING INFORMATION

Additional supporting information can be found online in the Supporting Information section at the end of this article.

How to cite this article: Rybinska I, Mangano N, Romero-Cordoba SL, et al. SAA1-dependent reprogramming of adipocytes by tumor cells is associated with triple negative breast cancer aggressiveness. *Int J Cancer*. 2024;1-15. doi:10.1002/ijc.34859